

# Primary Dendrite ARM Spacing Effects upon Mechanical Properties of an AL-3Wt% CU-1Wt% LI Alloy

G.A. Santos, P.R. Goulart, A.A. Couto and A. Garcia

**Abstract** The imposition of a wide range of operational conditions in foundry and castings processes generates, as a direct consequence, a diversity of solidification structures. It is well known that mechanical properties depend on solidification structures. The literature presents relationships between yield strength and grain size, such as the Hall-Petch's equation, or ultimate tensile strength and dendrite arm spacing. In this work, an Al-3wt%Cu-1wt%Li alloy was solidified under upward unsteady state heat flow conditions. Heat was directionally extracted only through a water-cooled bottom made of steel (SAE 1020). The aim of the present study is to obtain correlations between the as-cast microstructure, solidification thermal variables and mechanical properties of an Al-3wt%Cu-1wt%Li alloy casting. The results include tip growth rate ( $V_L$ ), cooling rate ( $\dot{T}$ ), primary dendrite arm spacing ( $\lambda_1$ ), ultimate tensile strength ( $\sigma_{UTS}$ ) and yield strength ( $\sigma_y$ ) as a function of solidification conditions imposed by the metal/mold system. It is found that the primary dendrite arm spacing decreases with the increase in tip growth rate and cooling rate. In both cases ( $\sigma_{UTS}$  and  $\sigma_y = 0.2 \text{ \%}\epsilon$ ), the finer dendritic arrangement presents superior mechanical properties.

---

G.A. Santos (✉) · P.R. Goulart

Department of Mechanical, Federal Institute of São Paulo, IFSP, São Paulo, SP, Brazil  
e-mail: givanildo@ifsp.edu.br

P.R. Goulart

e-mail: pedrogoulart1951@yahoo.com.br

A.A. Couto

Department of Materials Engineering, Institute of Nuclear and Energy Research, IPEN, São Paulo, SP, Brazil  
e-mail: acouto@ipen.br

A.A. Couto

Department of Materials Engineering, Mackenzie Presbyterian University, UPM, São Paulo, SP, Brazil

A. Garcia

Department of Materials Engineering, State University of Campinas, UNICAMP, Campinas, SP, Brazil  
e-mail: amaurig@fem.unicamp.br

© Springer Science+Business Media Singapore 2017

A. Öchsner and H. Altenbach (eds.), *Properties and Characterization of Modern Materials*, Advanced Structured Materials 33,  
DOI 10.1007/978-981-10-1602-8\_19

215

**Keywords** Al–3wt%Cu–1wt%Li alloy · Primary dendrite arm spacing · Solidification thermal variables · Mechanical properties

## 1 Introduction

The high specific properties of Al–Li alloys have led to tremendous development effort aimed in particular at aerospace applications. Al–Li castings and cast alloys that combine the good properties of Al–Li alloys with foundry technology have great potential in both the aircraft and automotive sectors [1]. To provide a basis for composition design of these alloys, a study on the solidification process, microstructure and mechanical properties of Al–Li cast alloys has been carried out.

Solidification of metals involves the transformation of the molten metal back into the solid state. The transformation of a liquid into solid is probably the most important phase transformation in applications of science and engineering materials. Casting of metals is an example of solidification process. The principle of casting seems simple: melt the metal, pour it into a mold, and let it cool and solidify; yet there are many factors and variables that must be considered in order to accomplish a successful casting operation. The physical mechanism of solidification that occurs during casting influences the structure and properties of metals [2].

The effects of microstructure on metallic alloys properties has been highlighted in various studies and particularly, the influence of grain size and dendrite arm spacing upon the mechanical properties has been reported [2–10]. Although the metallurgical and micromechanical aspects of the factors controlling microstructure, unsoundness, strength and ductility of as-cast alloys are complex, it is well known that solidification processing variables are of high importance. In the as-cast state an alloy may possess within individual grains, a dendritic network where solute concentration varies continuously, a complex dispersion of second phases and possibly porosity and inclusions [6]. In addition to the above obstacles to slip, the grain boundary is present at the grain perimeter. It is generally found that the grain size reduction increases the metal strength. The well known Hall-Petch equation shows that the yield strength is proportional to the reciprocal of the square root of the grain diameter [5].

For cast metals, however, it is not always true that the strength improves with decreasing grain size. Strength will increase with grain size reduction only if the production of small grains does not increase the amount of microporosity, the percentage volume of second phase or the dendrite spacing [6].

It is well known that there is a close correlation between thermal variables and the solidification structure and as a direct consequence, morphological structure parameters such as grain size and dendritic arm spacing also depend on solidification conditions imposed by the metal/mould system. Thus, the control of solidification thermal variables such as tip growth rate ( $V_L$ ) and cooling rate ( $\dot{T}$ ) permits

a range of microstructures to be obtained [11–19]. Reports can be found in the literature relating microstructural characteristics with mechanical properties (i.e., ultimate tensile strength, and yield strength) [2–10].

The present work focuses on the influence of heat transfer solidification variables on the microstructural formation of Al–3wt%Cu–1wt%Li alloy castings and on the development of correlations between dendritic spacing and mechanical properties. Experimental results include tip growth rate ( $V_L$ ) and cooling rate ( $\dot{T}$ ), primary dendrite arm spacing ( $\lambda_1$ ), ultimate tensile strength ( $\sigma_{UTS}$ ) and yield strength ( $\sigma_y$ ).

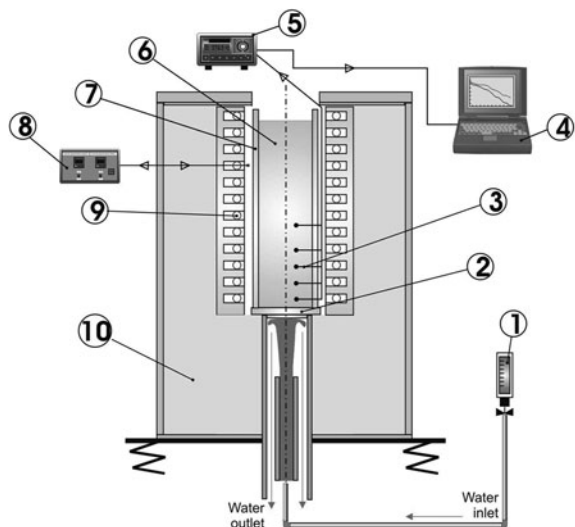
## 2 Materials and Methods

Figure 1 shows the casting assembly used in the experiments. It can be seen that heat is directionally extracted only through a water-cooled bottom made of steel, promoting vertical upward directional solidification. The use of bottoms made of low carbon steel (SAE 1020) permitted a wide range of solidification conditions to be analyzed. As a consequence, a wide range of dendritic spacings should be expected.

A stainless steel split mold was used having an internal diameter of 60 mm, height 157 mm and a 5 mm wall thickness. The lateral inner mold surface was covered with a layer of insulating alumina to minimize radial heat losses. The bottom part of the mold was closed with a thin (3 mm) steel sheet.

Experiments were performed with an Al–3wt%Cu–1wt%Li alloy. The mentioned chemistry was evaluated regarding to dendritic growth while tensile tests were performed with this aluminum alloy. The thermophysical properties of the aluminum and studied alloy are summarized in Table 1. Specific heats, latent heats

**Fig. 1** Schematic representation of the experimental setup: 1 rotameter; 2 heat-extracting bottom; 3 thermocouples; 4 computer and data acquisition software; 5 data logger; 6 casting; 7 mold; 8 temperature controller; 9 electric heaters; 10 insulating ceramic shielding

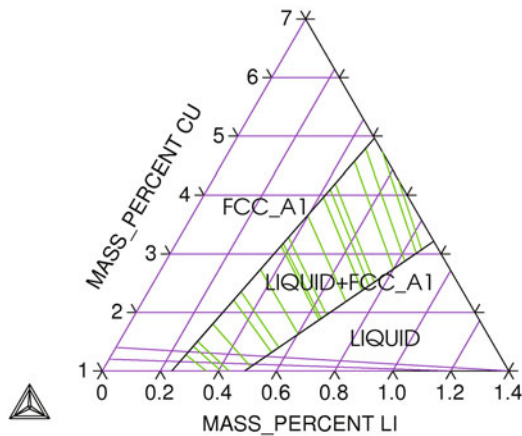


**Table 1** Casting material used for experimentation and the corresponding thermophysical properties

Properties	Symbol/units	Al (pure)	Al-3wt%Cu-1wt%Li
Thermal conductivity	$K_S$ [W m <sup>-1</sup> K <sup>-1</sup> ]	221.6	216
	$K_L$ [W m <sup>-1</sup> K <sup>-1</sup> ]	91.9	93
Specific heat	$c_S$ [J kg <sup>-1</sup> K <sup>-1</sup> ]	1255	1170
	$c_L$ [J kg <sup>-1</sup> K <sup>-1</sup> ]	1175	1140
Density	$\rho_S$ [kg m <sup>-3</sup> ]	2700	2887
	$\rho_L$ [kg m <sup>-3</sup> ]	2389	2554
Latent heat of fusion	$L$ [J kg <sup>-1</sup> ]	383,000	322,000
Melting temperature	$T_M$ [°C]	660	
Liquidus temperature	$T_{Liq}$ [°C]		655
Solidus temperature	$T_{Sol}$ [°C]		645

**Fig. 2** Al-Cu-Li partial phase diagram furnished by the software ThermoCalc AB, version N

THERMO-CALC (2009.06.04:13.44) :AL-CU-LI at T=930 K  
 DATABASE:PURE4  
 T=930, P=1E5, N=1;

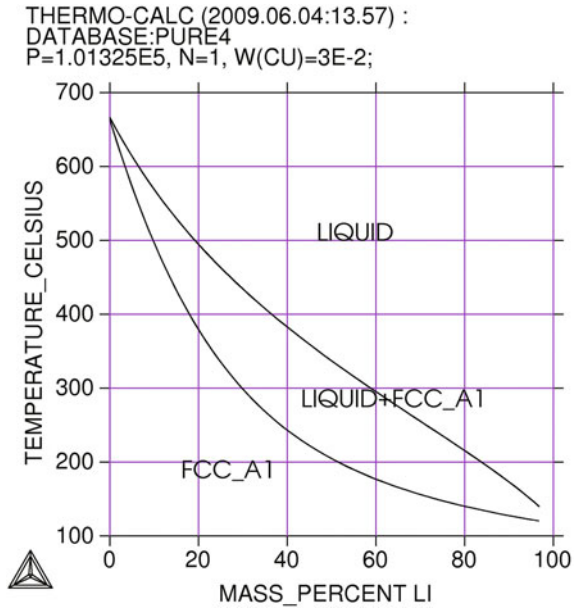


of fusion and *liquidus* temperatures were obtained by Thermo-Calc<sup>1</sup> computations. The Al-Cu-Li partial phase diagram and the Al-Cu-Li isomorph phase diagram with 3wt% Cu (constant) were also computed by Thermo-Calc and it is shown in Figs. 2 and 3, respectively.

The initial melt temperature ( $T_p$ ) was standardized at 10 °C above the *liquidus* temperature ( $T_{Liq}$ ) of the studied alloy. The thermal contact condition at the metal/mold interface was also standardized with the heat-extracting surface at the mold bottom being polished.

<sup>1</sup>Thermo-Calc software is an exclusive copyright property of the STT Foundation (Foundation of Computational Thermodynamics, Stockholm, Sweden).

**Fig. 3** Al-Cu-Li isomorph phase diagram with 3wt% Cu (constant) furnished by the software ThermoCalc AB, version N



Continuous temperature measurements in the casting were monitored during solidification via the output of a bank of fine type K thermocouples (made from 0.2 mm diameter wire) sheathed in 1.6 mm diameter steel tubes, and positioned at 4, 8, 12, 22, 52, 68 and 88 mm from the heat-extracting surface at the bottom. The thermocouples were calibrated at the melting point of aluminum exhibiting fluctuations of about 1 °C. All of the thermocouples were connected by coaxial cables to a data logger interfaced with a computer, and the temperature data, read at intervals of 0.1 s, were automatically acquired.

Each cylindrical ingot was subsequently sectioned along its vertical axis, ground and etched with an acid solution to reveal the macrostructure (Poulton’s reagent: 5 mL H<sub>2</sub>O; 5 mL HF—48 %; 30 mL HNO<sub>3</sub>; 60 mL HCl).

Selected transverse (perpendicular to the growth direction) sections of the directionally solidified specimens at different positions from the metal/mold interface were polished and etched with Tucker’s reagent (a solution of 45 mL HCl; 15 mL HNO<sub>3</sub>, 15 mL HF and 25 mL distilled water) for metallography. Image processing systems Neophot 32 (Carl Zeiss, Esslingen, Germany) and Leica Quantimet 500 MC (Leica Imaging Systems Ltd., Cambridge, England) were used to measure primary dendrite arm spacings,  $\lambda_1$ , (about 30 independent readings for each selected position, with the average taken to be the local spacing) and their distribution range. The method used for measuring the primary arm spacing on the transverse section was the triangle method [13].

Transverse specimens were cut from the castings, as indicated in Fig. 4, and prepared for tensile testing according to specifications of ASTM standard E 8M [20]. In order to ensure reproducibility of results, three specimens were tested for each

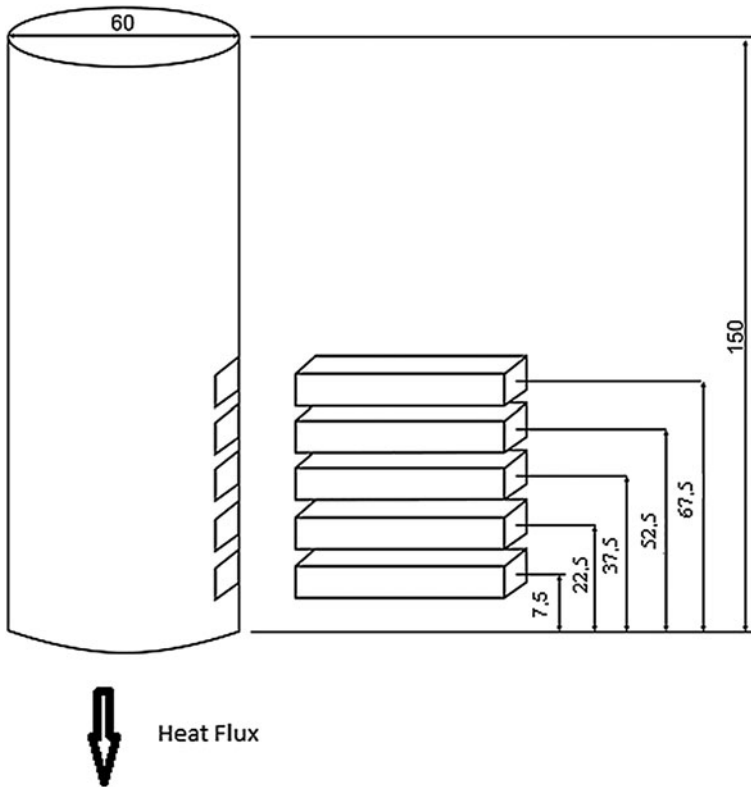


Fig. 4 Removal of specimens for tensile tests (dimensions in mm)

selected position, and mean values of yield tensile strength, ultimate tensile strength have been determined at different positions with respect to the casting surface.

### 3 Results and Discussion

Figure 5 shows cooling curves corresponding to the thermal responses of seven thermocouples inserted into the casting at different positions from the cooled surface. The data were acquired during the solidification of Al–3wt%Cu–1wt%Li alloy.

The thermocouples readings have been used to generate a plot of position from the metal/mold interface as a function of time corresponding to the *liquidus* ( $t_L$ ) front passing by each thermocouple. A curve fitting technique on these experimental points has generated a power function of position as a function of time (Fig. 6).

The derivative of this function with respect to time has yielded values for tip growth rate,  $V_L = dP/dt$ . Figure 7 shows the experiment performed with an Al–3wt% Cu–1wt%Li alloy. The line represents an empirical power function fit with the experimental points. A single experimental law represents the experimental scatter (Fig. 8).

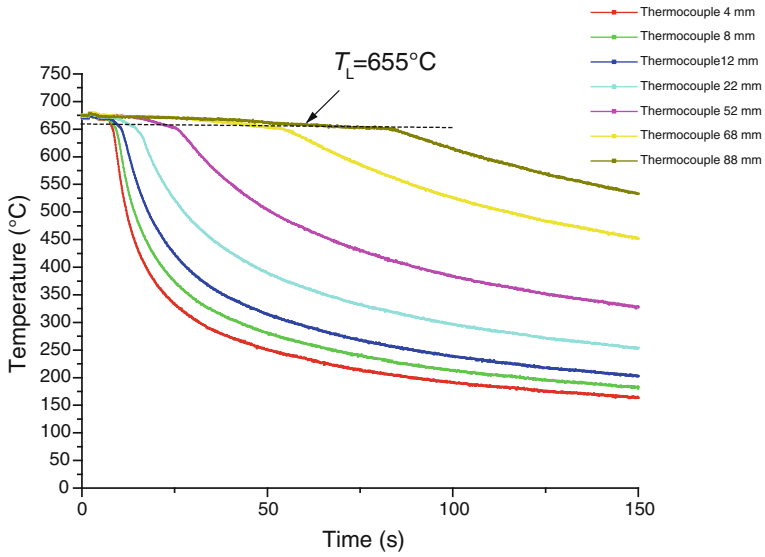


**Fig. 5** Experimental cooling curves for seven thermocouples inside the casting (Al-3wt%Cu-1wt%Li)

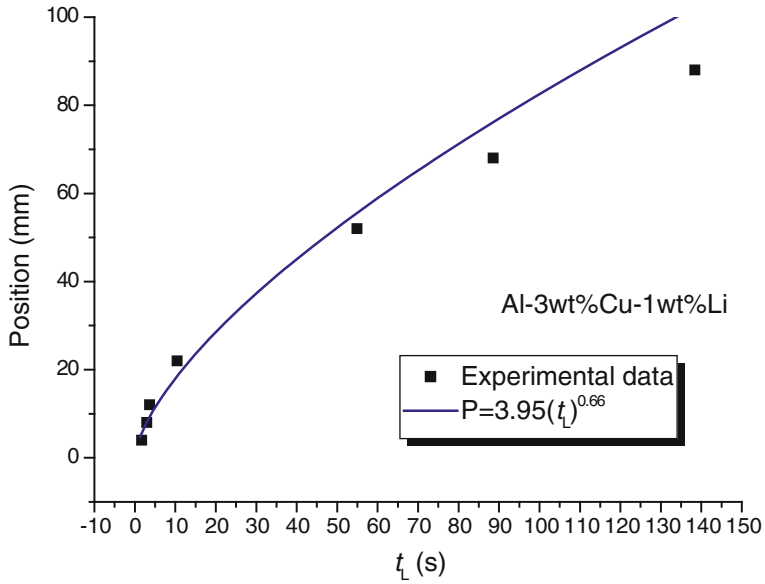


**Fig. 6** Position from the metal/mold interface as a function of time corresponding to the *liquidus* ( $t_L$ ) for thermocouples inside the casting (Al-3wt%Cu-1wt%Li)

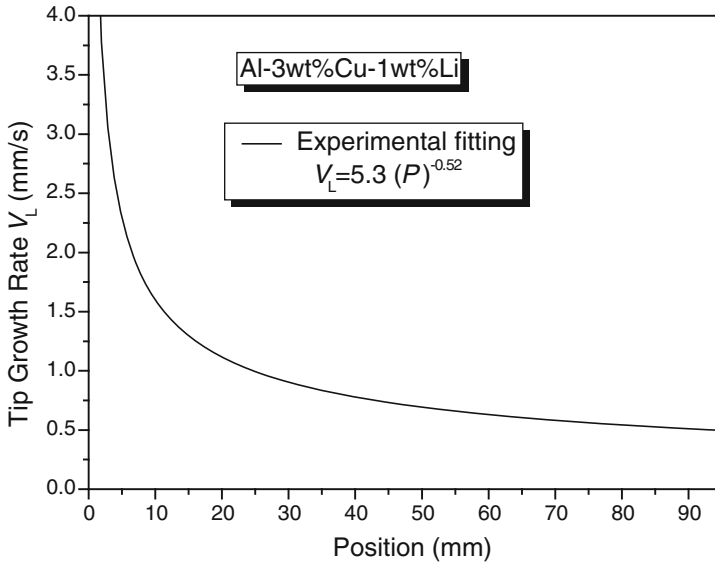


**Fig. 7** Tip growth rate as a function of position from the metal/mold interface for an Al-3wt%Cu-1wt%Li alloy

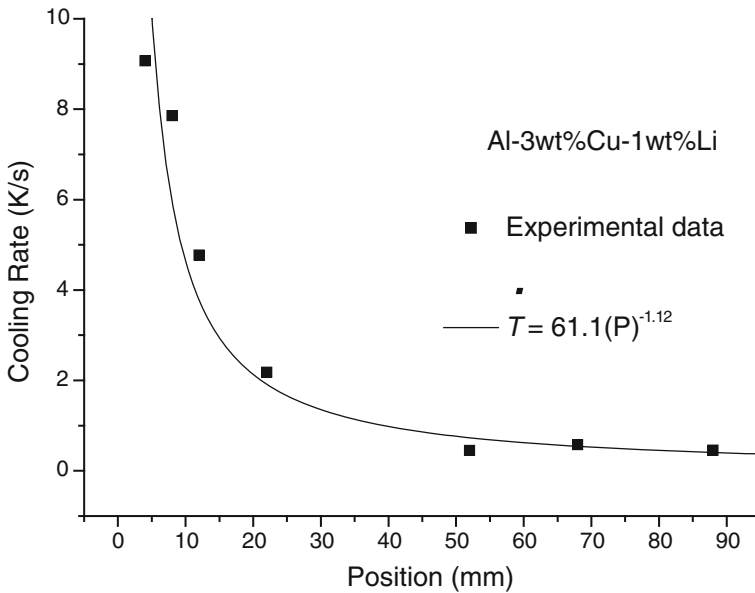


**Fig. 8** Cooling rate as a function of position from the metal/mold interface for an Al-3wt%Cu-1wt%Li alloy



**Fig. 9** Macrostructure of Al-3wt%Cu-1wt%Li alloy casting

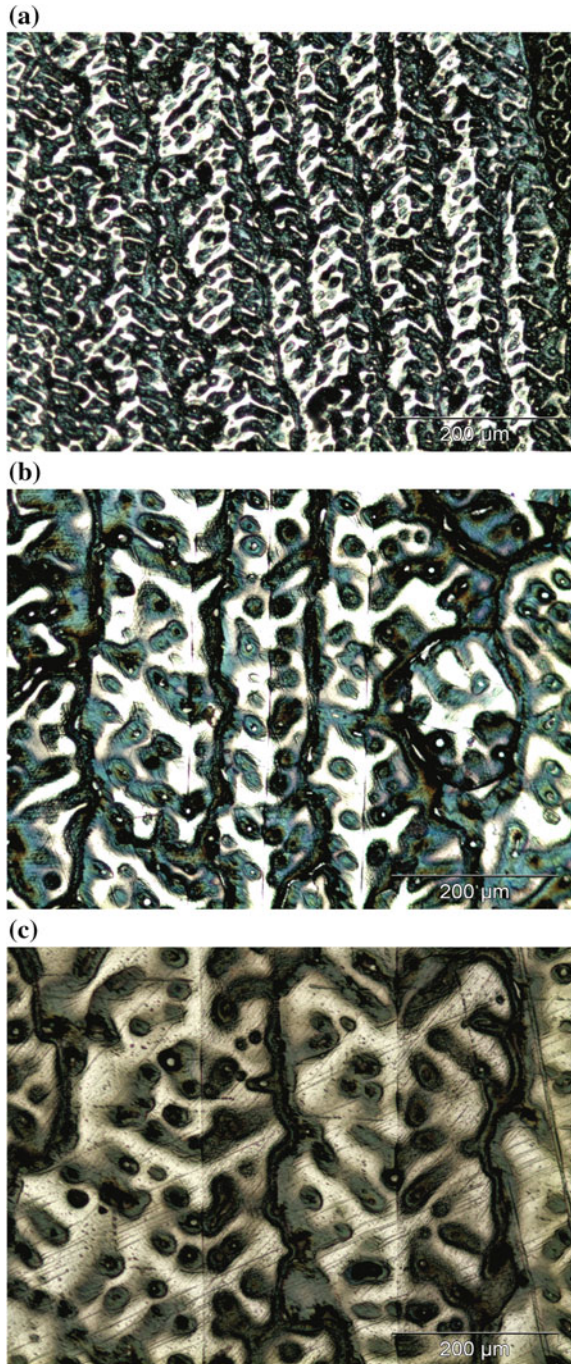


The data acquisition system, in which temperature readings are collected at a frequency of 0.5 s, permits accurate determination of the slope of the experimental cooling curves. The cooling rate was determined by considering the thermal data recorded immediately after the passing of the *liquidus* front by each thermocouple.

The macrostructure of the directionally solidified casting are shown in Fig. 9. Columnar growth has prevailed along the casting length for the alloy experimentally examined.

Typical microstructures on transverse sections of Al-3wt%Cu-1wt%Li alloy casting are shown in Fig. 10. The dendrite arm spacings were sufficiently distinct to permit accurate measurements along the casting length.

**Fig. 10** Experimental  $\lambda_1$  at different positions from the casting surface for the Al-3wt%Cu-1wt%Li alloy: 10 mm (a), 30 mm (b) and 60 mm (c)



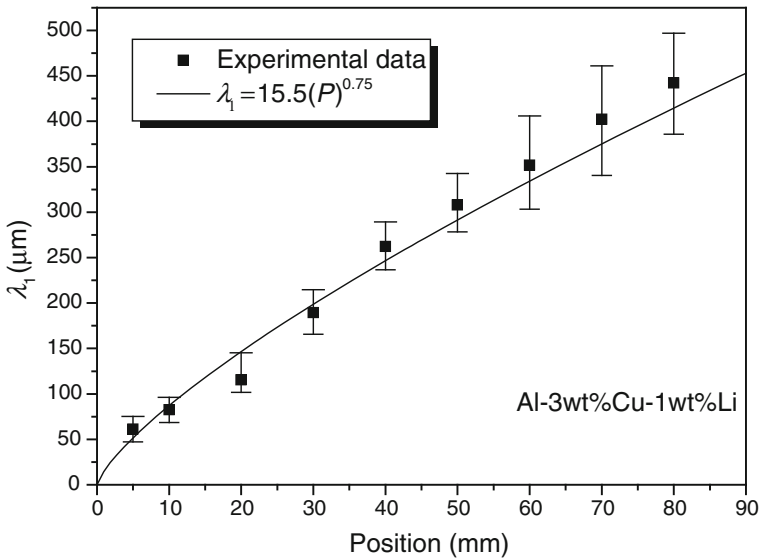


**Fig. 11** Primary dendrite arm spacing as a function of position from the metal/mold interface for an Al-3wt%Cu-1wt%Li alloy

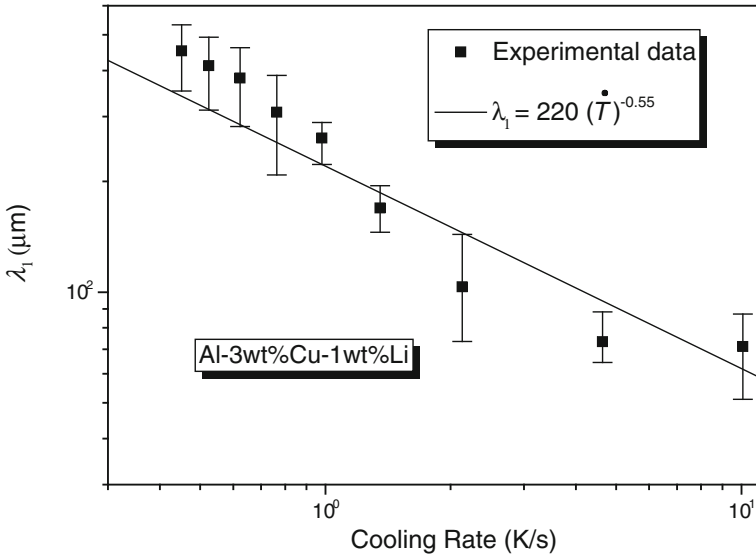
Figure 11 shows the measured primary dendrite arm spacing ( $\lambda_1$ ) expressed as a function of distance from the metal/mold interface. It can be observed that, as expected,  $\lambda_1$  increases with distance from casting surface due to the corresponding decrease in cooling rate and tip growth rate.

Figures 12 and 13 show the mean experimental values of primary dendrite arm spacings ( $\lambda_1$ ) as a function of cooling rate and tip growth rate, respectively, measured from the afore mentioned microstructures. Points are experimental results and lines represent an empirical fit of the experimental points, with dendritic spacings being expressed as a power function either of tip growth rate or of cooling rate.

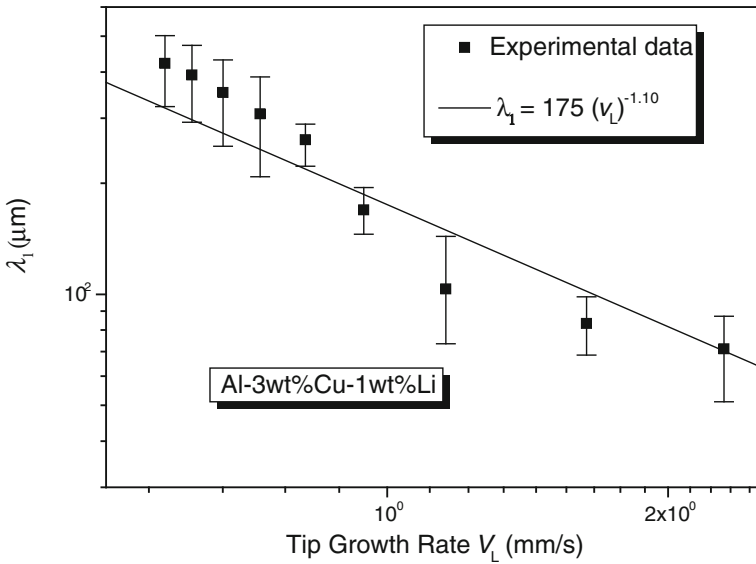
It can be seen that a  $-0.55$  power law characterizes the experimental variation of primary spacings with cooling rate (Fig. 12). This is in agreement with recent observations reported by Rocha et al. [13] that exponential relationships best generate the experimental variation of primary dendritic arms with cooling rate along the unsteady-state solidification of Sn-Pb and Al-Cu alloys. Peres and co-authors [21] have also found this type of relation as the best one regarding to unsteady-state directional solidification of Al-Si hypoeutectic alloys.

Figure 14 shows the primary dendrite stems have grown perpendicularly to the imposed loading in the tests, which probably becomes the primary dendrite an efficient barrier against the tensile forces. Because of that, the mechanical parameters determined through the tensile tests were correlated with primary dendrite arm spacing.

The results of the tensile tests are summarized in Fig. 15a, b, where the ultimate tensile strength ( $\sigma_{UTS}$ ) and the yield strength [ $\sigma_{y=0.2}$ ] (0.2 % proof stress) are related



**Fig. 12** Primary dendrite arm spacing as a function of cooling rate for an Al-3wt%Cu-1wt%Li alloy



**Fig. 13** Primary dendrite arm spacing as a function of tip growth rate for an Al-3wt%Cu-1wt%Li alloy

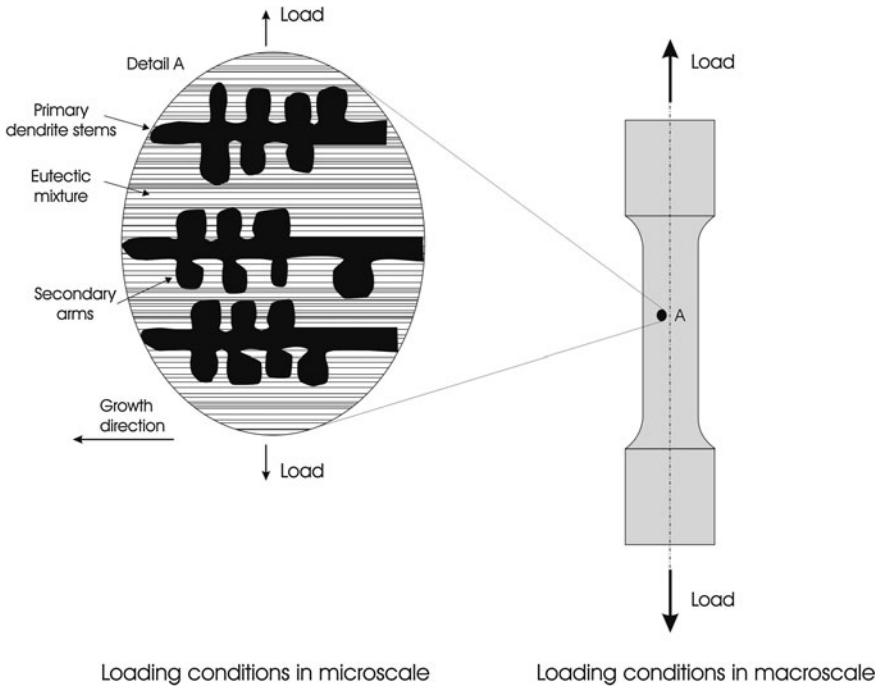


**Fig. 14** Aligned dendritic network dealing with the uniaxial loading of tensile tests

to the primary dendrite arm spacing, respectively. It can be seen that both  $\sigma_{UTS}$  and  $\sigma_y$  increase with decreasing dendrite arm spacing.

## 4 Conclusions

In order to investigate the role of primary dendrite arm spacing on mechanical properties of the Al-3wt%Cu-1wt%Li alloy, solidification experiments and tensile tests were carried out. The following main conclusions can be drawn from the present experimental investigation:

- (1) The experimental expressions correlating the ultimate tensile strength and yield strength with primary dendrite arm spacing for an Al-3wt%Cu-1wt%Li alloy have shown that a finer structural dendritic morphology provides better mechanical properties than a coarser morphology; and
- (2) The control of as-cast microstructures, by manipulating solidification processing variables, such the cooling rate and tip growth rate can be used as an alternative way to produce components with better mechanical properties.

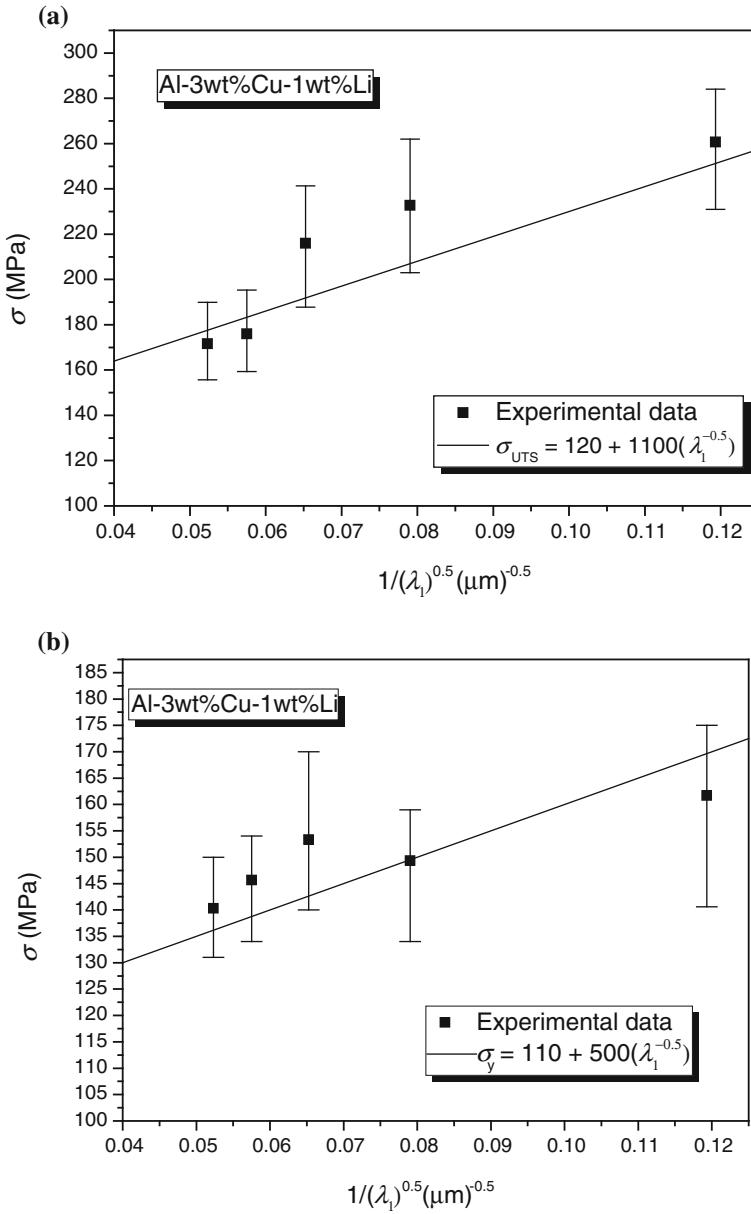


**Fig. 15** Relationships: **a** ultimate tensile strength  $\sigma_{UTS} = f(\lambda_1)$  and **b** yield strength  $\sigma_y = f(\lambda_1)$

## References

1. Wang C, Min G, Lu Q, Lu Z (2004) Solidification structure and mechanical properties of Al–Li–Cu–Zr cast alloys. *Int J Cast Metal Res* 17:264–266
2. Santos GA (2015) *Tecnologia dos materiais metálicos – propriedades, estruturas e processos de Obtenção*, 1st edn. Editora Érica Ltda, São Paulo
3. Garcia A (2007) *Solidificação: fundamentos e aplicações*, 2nd edn. Unicamp, Campinas
4. Park C, Kim S, Kwon Y, Lee Y, Lee J (2005) Mechanical and corrosion properties of rheocast and low-pressure cast A356-T6 alloy. *Mater Sci Eng* 391A:86–94
5. Petch NJ (1953) The cleavage strength of polycrystals. *J Iron Steel Inst* 174:25–28
6. Osório WRR, Garcia A (2002) Modeling dendritic structure and mechanical properties of Zn–Al alloys as a function of solidification conditions. *Mater Sci Eng* A325:103–111
7. Osório WRR, Leiva DR, Peixoto LC, Garcia LR, Garcia A (2013) Mechanical properties of Sn–Ag lead-free solder alloys based on the dendritic array and Ag<sub>3</sub>Sn morphology. *J Alloy Compd* 562:194–204
8. Osório WRR, Bortolozo AD, Peixoto LC, Garcia A (2014) Mechanical performance and microstructure array of as-cast lead–silver and lead–bismuth alloys. *J Power Sources (Print)* 271:124–133
9. Santos GA, Osório WRR, Garcia A, Neto CM, Goulart PR (2006) Effect of dendritic arm spacing on mechanical properties and corrosion resistance of Al 9wt pct Si and Zn 27wt pct Al alloys. *Metall Mater Trans A* 37:2525–2538
10. Santos GA, Neto CM, Osório WRR, Garcia A (2007) Design of mechanical properties of a Zn27Al alloy based on microstructure dendritic array spacing. *Mater Design* 28:2425–2430
11. Quaresma JMV, Santos CA, Garcia A (2000) Correlation between unsteady-state solidification conditions, dendrite spacings and mechanical properties of Al–Cu alloys. *Metall Mat Trans A* 31:3167–3178
12. Siqueira CA, Cheung N, Garcia A (2002) Solidification thermal parameters affecting the columnar-to-equiaxed transition. *Metall Mat Trans A* 33(7):2107–2118
13. Rocha OL, Siqueira CA, Garcia A (2003) Heat flow parameters affecting dendrite spacings during unsteady-state solidification of Sn–Pb and Al–Cu alloys. *Metall Mat Trans A* 34 (4):995–1006
14. Spinelli JE, Garcia A (2014) Development of solidification microstructure and tensile mechanical properties of Sn–0.7Cu and Sn–0.7Cu–2.0Ag solders. *J Mat Sci-Mat El* 25:478–486
15. Spinelli JE, Silva B, Garcia A (2014) Assessment of tertiary dendritic growth and its effects on mechanical properties of directionally solidified Sn–0.7Cu–xAg solder alloys. *J Electron Mater* 1347–1361
16. Brito C, Costa TA, Vida TA, Bertelli F, Cheung N, Spinelli JE, Garcia A (2015) Characterization of dendritic microstructure, intermetallic phases, and hardness of directionally solidified Al–Mg and Al–Mg–Si alloys. *Metall Mat Trans A* 3343–3355
17. Brito C, Reinhart G, Nguyen-Thi H, Mangelinck-Noel N, Cheung N, Spinelli JE, Garcia A (2015) High cooling rate cells, dendrites, microstructural spacings and microhardness in a directionally solidified Al–Mg–Si alloy. *J Alloy Compd* 145–149
18. Dias M, Costa TA, Rocha OFL, Spinelli JE, Garcia A (2015) Interconnection of thermal parameters, microstructure and mechanical properties in directionally solidified Sn–Sb lead-free solder alloys. *Mater Charact* 106:52–61
19. Silva B, Nguyen-Thi H, Reinhart G, Mangelinck-Noel N, Garcia A, Spinelli JE (2015) Microstructural development and mechanical properties of a near-eutectic directionally solidified Sn–Bi solder alloy. *Mater Charact* 107:43–53
20. ASTM E 8M (1995) Standard test methods for tension testing of metallic materials. ASTM
21. Peres MD, Siqueira CA, Garcia A (2004) Macrostructural and microstructural development in Al–Si alloys directionally solidified under unsteady-state conditions. *J Alloy Compd* 381:168–181